Proceedings of the 9th World Congress on New Technologies (NewTech'23)
Brunel University, London, United Kingdom - August 09-11, 2023
Paper No. ICNFA 108
DOI: 10.11159/icnfa23.108

Nano Phase-containing Al-0.3Mn Alloy for Potential EV Applications: Microstructure, Tensile Behavior and Electrical Conductivity

Wutian Shen, Anita Hu, Jun Wang, Ali Dhaif, Henry Hu
Department of Mechanical, Automotive and Materials Engineering, University of Windsor
Windsor, Ontario Canada N9B3P4
shen12a@uwindsor.ca; hu14l@uwindsor.ca; jun.wang@uwindsor.ca; dhaifa@uwindsor.ca; huh@uwindsor.ca

Abstract **-** An Al alloy containing 0.3 wt% Mn (Al-0.3Mn) for potential applications in electric vehicles (EV) was prepared by permanent steel mold casting (PSMC) along with high purity (HP) Al (99.9%). The microstructure of the as-cast Al-0.3Mn alloy was analyzed by scanning electron microscopy (SEM) and energy dispersive spectroscopy (EDS). The microstructure analyses revealed that the Al-0.3Mn alloy consisted of primary Al phase, micron-sized Al-Fe-Mn intermetallic phase, and nano-sized Al-Mn intermetallic phase. The tensile properties including ultimate tensile strength (UTS), yield strength (YS) and elongation (e_f) were evaluated by tensile testing. The phase sensitive eddy current method was employed to measure the electrical conductivity. The addition of 0.3 wt% Mn increased both the UTS and YS of the cast HP Al significantly to 72.3 and 20.4 MPa from 59.2 and 14.0 MPa. The evaluation of tensile behaviors indicated that the Mn addition significantly improved the resilience and strain hardening rate of the PSMC HP Al, although the toughness of the PSMC Al-0.3Mn was comparable to that of PSMC HP Al. However, the e_f and electrical conductivity of the cast alloy decreased to 28.9% and 45.6 %IACS from 37.1% and 61.1 %IACS. The difference in tensile behaviors and electrical conductivities between the PSMC Al-0.3Mn alloy and the PSMC HP Al should be attribute to the emergence of a large amount (2.1%) of the micron Al-Fe-Mn and nano Al-Mn intermetallic phases in the PSMC Al-0.3Mn alloy, compared to only 0.4% of Al-Fe intermetallics in the PSMC HP Al.

Keywords**:** nano intermetallic phases, Al-Mn alloys, microstructure, tensile behavior, electrical conductivity, electric motor, electric vehicle, permanent mold casting.

1. Introduction

To reduce greenhouse gas emissions, battery-powered electric vehicles (BEVs) are gaining the popularity in the auto community. For further expansion of the BEV market, development of inexpensive, lightweight, highly efficient induction motors becomes an urgent task the automotive industry to, since the current BEVs are considerably heavier than those gasoline-powered vehicles (GPVs). In induction motors, squirrel cage rotors play a key role in electromechanical energy conversion [1-3]. At present, pure Al as a substitute for copper is used for production of rotor bars in induction motors by casting because of its high electrical conductivity, lightweight and low price. Unfortunately, the tensile properties including the ultimate tensile strength (UTS) and yield strength (YS) of the pure aluminum are very low. The engineering performance assurance of Al rotor bars requires a large cooling system to be placed in the induction motor. The installation of the cooling system enlarges the size and makes the induction motor much heavy, and consequently increases the BEV weight [1]. A reduction in the BEV weight becomes essential for low battery energy consumption and long driving range [3].

The employment of conventional Al casting alloys for the rotor bar could eliminate the large cooling system and reduce the motor weight. However, commercially available Al casting alloys containing Si, Mg and Cu exhibit low electrical conductivities around 30 %IACS, because they have high solubilities in aluminum solid solution [4-11]. Manganese as a low-cost transition metal has a multifaceted array of industrial alloy uses in ferrous alloys-steels and cast iron, which can improve their strength, workability, and wear resistance. The 3xxx series of wrought Al alloys employs Mn as a major alloying element, and are used for applications, in which moderate strength combined with high ductility and excellent corrosion resistance is required. With low weight percent of Mn addition, the YS and UTS of Al alloys increase without sacrificing ductility, as Mn in aluminum-rich alloys forms a manganese dispersoid of Al_6Mn, which blocks the dislocation and changes the slip system by means of cross-slip [7]. Compared to common alloying elements, Si, Cu and Mg, Mn has a low solubility in pure aluminum, which could minimize the reduction in electrical conductivity. The maximum solubility of Mn is 1.25 wt% at 658 ^oC [7, 8]. As a result, low Mn addition

enables the development of low-cost Al alloys with not only high strengths but also high electrical conductivities, which are required for applications in BEVs. However, simultaneous studies on microstructure, tensile behavior and electrical conductivities of castable Al-Mn alloys are scarce.

In the present study, an Al-0.3Mn alloy and HP Al (99.9%) were cast in a permanent steel mold (PSMC) to produce retangular casting plates. The mechanical properties and the electrical conductivities of the prepared castings were evaluated. The preliminary microstructure analyses of the PSMC Al-0.3Mn alloy and HP Al was carried out. printer.

2. Experimental Procedure

2.1. Materials and Casting

The Al-0.3Mn alloy with the chemical composition in Table 1 was selected for investigation. High purity (HP) Al (99.9%) was also used for the purpose of comparison, of which composition is given in Table 1. In each casting run, about 1 kg of the alloy melt was prepared in an electric resistance furnace using a graphite crucible. The melt was held at 750 ℃ ±10 ℃ for about 20 min, stirred for 10 minute to homogenize its chemical composition, and then poured into a permanent steel mold to produce a rectangular casting plate with the dimensions of 150 mm × 125 mm × 10 mm.

Table 1 Chemical compositions of Al-0.3Mn alloy and high purity (HP) Al

Materials	chemical composition (wt%)							
	Mn	Fe	Si	Cu	Zn	C	Al	Others
Al-0.3Mn	0.30	0.034	0.062	<0.002	<0.01	<0.01	remain	None
HP Al	-	0.030	0.060	-	0.001	<0.01	99.9%	0.13

2.2. Porosity Measurement

Porosity was quantitatively determined by density measurements. Based on the weight measurement of both the permanent steel mold cast (PSMC) Al-0.3Mn and PSMC HP Al specimens in air and water, the actual density (D_a) of each specimen was determined using Archimedes principle based on ASTM Standard D3800 [12]

$$D_a = \frac{D_w W_a}{W_a - W_w} \quad \text{(Eq 1)}$$

where W_a and W_w are the weight of the specimen in the air and in the water, respectively, and D_w the density of water. The porosity of each specimen was calculated by the following equation. The porosity of each specimen was calculated by the density values through the following equation (ASTM C948) [13]

$$\%\ Porosity = \left[\frac{D_t - D_a}{D_t}\right] \times 100\% \quad \text{(Eq 2)}$$

where D_t is the theoretical densities of the pure Al, with the density of 2.70 g/cm^3 [9], and the Al-0.3Mn alloy calculated based on the weight percentages of Al (2.70 g/cm^3) and Mn (7.43 g/cm^3), with the density of 2.72 g/cm^3.

2.3. Microstructure Analysis

Metallographic samples were cut from the center of cast specimens. The standard mounting and polishing procedure were applied to the cut metallographic samples subsequently before the observation. The detailed features of the microstructure were characterized by a scanning electron microscope (SEM), Hitachi™ Tabletop Microscope TM3000 (Tokyo, Japan), with a maximum resolution of 30 nm in a backscattered mode/1 μm in x-ray diffraction mapping mode, and useful magnification of 10 to 10,000. maximize composition reading of the energy dispersive spectroscopy (EDS) data. Quantitative evaluation of specimen microstructures consisted of calculating area fractions of different phase constituents and porosity. This procedure was completed with ImageJ, a public domain image processing system [14].

2.4. Tensile Testing

The mechanical properties of both the PSMC Al-0.3Mn and PSMC HP Al specimens were evaluated by the tensile testing, which was carried out at ambient temperature on a MTS Criterion (Model 43) Tensile Test Machine (Eden Prairie, MN, USA) equipped with a data acquisition system. According to ASTM B557 [15], subsize flat tensile specimens (0.025 m in gage length, 0.006 m in width, and 0.010 m in as-cast thickness) were machined from the sectioned coupons. The strain rate during tensile testing was 0.5 mm/min with a sampling rate of 10 Hz. The tensile properties, including 0.2% yield strength (YS), ultimate tensile strength (UTS), elongation to failure (e_f), and elastic modulus (E) were obtained based on the average of three tests.

2.5. Measurement of Electrical Conductivity

The electrical conductivity is an important electrical property of the both the PSMC Al-0.3Mn alloy and PSMC HP Al specimens. The handhold device SIGMASCOPE with FS40 probe was employed to perform the electrical conductivity measurements of the the PSMC Al-0.3Mn alloy and PSMC HP Al specimens based on the phase sensitive eddy current method. This type of signal evaluation enables non-contact measurement. It also minimizes the influence of surface roughness. The measuring range of the device is 0.5 - 108% IACS (% International Annealed Copper Standard), and the accuracy at room temperature is ± 0.5% of the measured reading. The minimum measurable radius of the specimen was 7 mm. The electrical conductivity data were obtained based on the average of three tests.

3. Results and Discussion

3.1. Microstructure

Figure 1 presents SEM micrographs and EDS spectra showing the microstructural constituents of the permanent steel mod cast (PSMC) Al-0.3% Mn alloy and PSMC HP Al. The microstructure of the PSMC Al-0.3Mn alloy mainly consisted of not only the primary α-Al phase (gray) but also the micron Al-Fe-Mn intermetallic phases and nano Al-Mn imtermetallic phase (white). The observation on the element distribution and phase morphology in areas A, B and C implied the presence of the primary Al phase as matrix and the intermetallic phases in the form of precipitates as indicated in Figure 1(a)-(d).

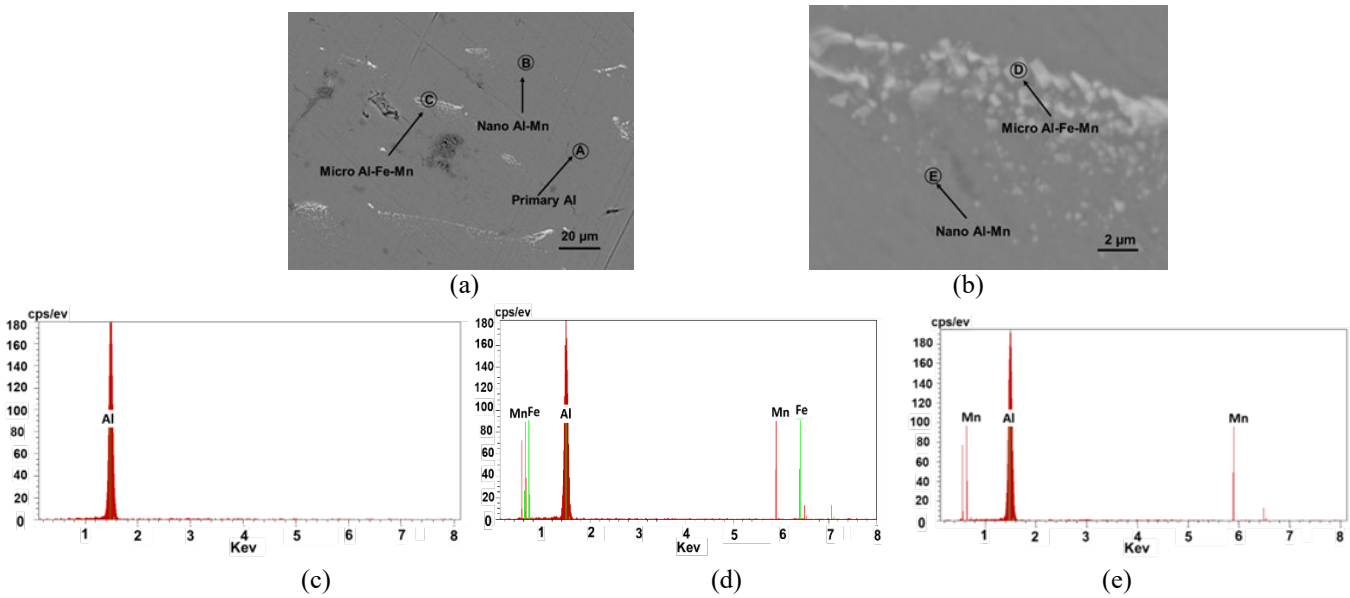

Fig. 1: SEM micrographs showing microstructure of PSMC Al-0.3Mn alloy, (a) low and (b) high magnifications, and EDS spectra identifying (c) primary Al phase, (d) micron Al-Fe-Mn phase, and (e) nano Al-Mn phase.

Also, according to the SEM and EDS analyses, nano Al-Mn particles were identified besides the micron-sized Al-Fe-Mn phase as can be seen from areas E and D in Figure 1 (b). The examination of the SEM micrograph also revealed the presence of porosity (dark gray), due to the poor feedability of the PSMC Al-0.3Mn alloy.

Figure 2 gives SEM micrograph and EDS spectra for the PSMC HP Al. Compare to that of the PSMC Al-0.3Mn alloy, the microstructure of the PSMC HP Al was comprised of different phases and porosity. The microstructural constituents were identified by the EDS spectra given in Figure 2 (c) and (d). It was revealed that the primary Al (gray), and micron Al-Fe and nano Al-Fe intermetallic phases (white) were present in the microstructure. The porosity was also observed due to the poor castability of the HP Al.

To determine the area fractions of the intermetallic phases, ImageJ was used to convert the SEM micrographs to binary and white images, with the black areas representing the intermetallic phases (Al-Fe-Mn, Al-Fe and Al-Mn phases) and the white areas representing primary α-Al. Following conversion, the software automatically calculated area fractions of black and white areas. Figure 3 presents the converted micrographs highlighting the presence of the intermetallic phases in the observed PSMC Al-0.3Mn alloy and HP Al represented by the black areas. Figure 4 shows the area fractions of the intermetallic phases. The area fractions of the intermetallic phases in the PSMC Al-0.3Mn alloy and the PSMC HP Al were measured to be 2.1 and 0.4% , respectively.

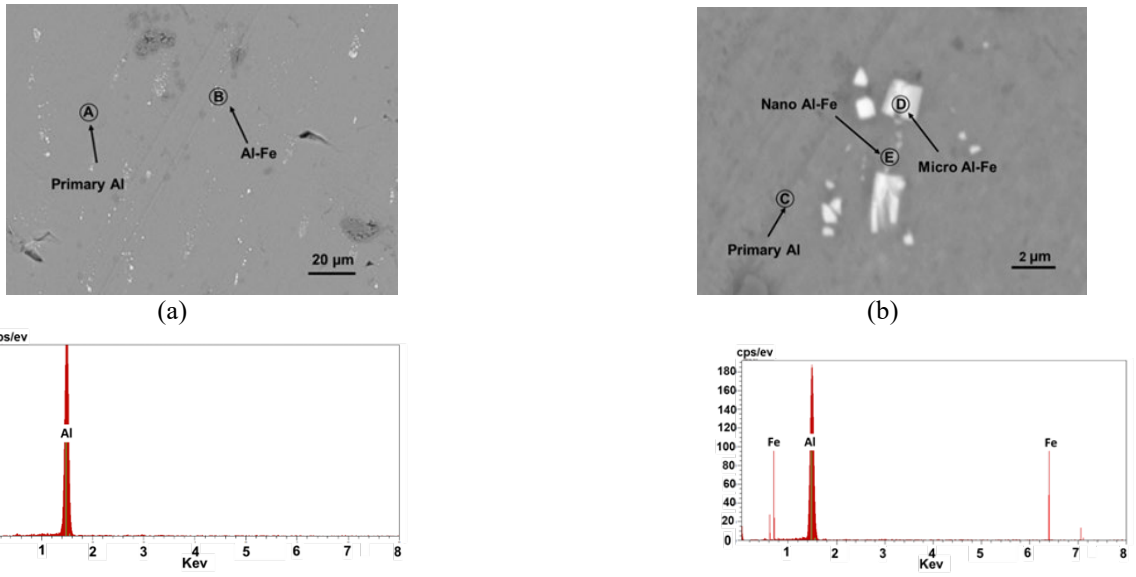

(a) (b)

(c) (d)

Fig. 2: SEM micrograph showing microstructure of PSMC HP Al (99.9%), (a) low (b) high magnifications, and EDS spectra identifying (c) primary Al phase, (d) Al-Fe intermetallic phase,

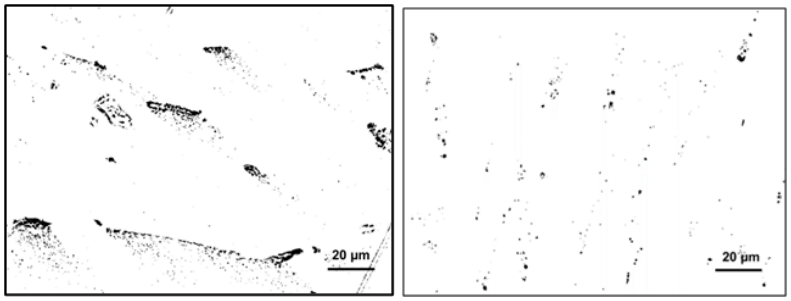

(a) (b)

Fig. 3: Micrographs in binary black and white images showing the contents of imtermetallics in (a) the PSMC Al-0.3% Mn alloy and (b) the PSMC HP Al.

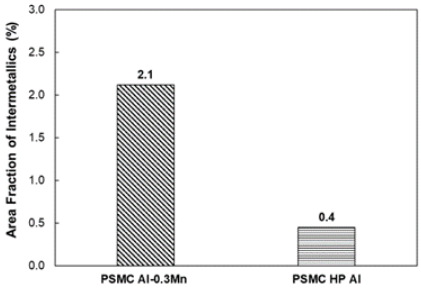

Fig. 4: Area Fractions of the PSMC Al-0.3Mn alloy and CP Al (99.9%).

3.2. Porosity Evaluation

Figure 5 presents the binary black and white images converted from the SEM micrographs by ImageJ, showing the porosity contents in the PSMC Al-0.3Mn alloy and PSMC HP Al. It is worthwhile noting that both the PSMC Al-0.3Mn alloy and the HP Al were cast in the steel mold with the cross-section thickness of 10 mm, which suggested they were cooled in a relatively slow rate. Therefore, these two materials exhibited the large number of gas and shrinkage pores (black area). The porosities of the PSMC Al-0.3Mn alloy and the PSMC HP Al alloys determined quantitatively from the density measurements and the imageJ analyses are shown in Figure 6. The porosity of the PSMC Al-0.3Mn alloy was around 2.26% from the density measurement and 2.12% from the imageJ. The PSMC HP Al had a porosity level of 2.25% from the imageJ, which was similar with that (2.26%) of the PSMC Al-0.3Mn alloy.

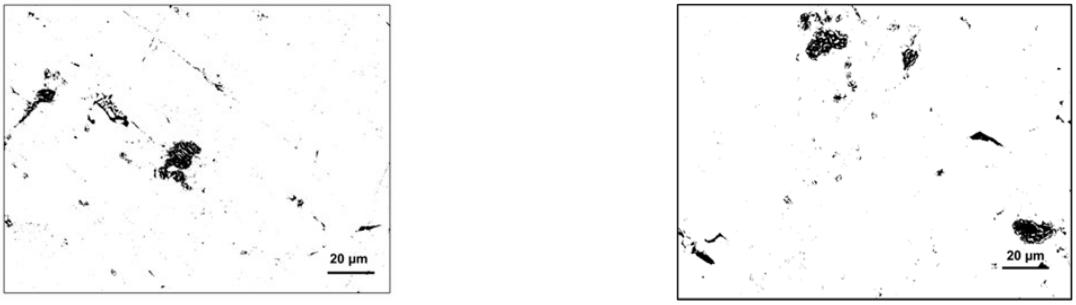

(a) (b)

Fig. 5: Binary black and white images showing porosity in (a) PSMC Al-0.3Mn alloy and (b) PSMC HP Al.

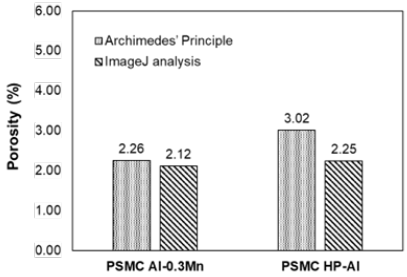

Fig. 6: Porosity contents of the PSMC Al-0.3Mn alloy and HP Al (99.9%).

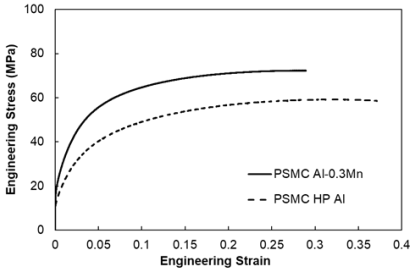

Fig. 7: Typical engineering stress vs. strain curves of the PSMC Al-0.3Mn alloy and PSMC HP Al.

Table 2. Tensile properties of the PSMC Al-0.3Mn alloy and PSMC HP Al (99.9%) at room temperature

Material	UTS (MPa)	YS (MPa)	e_f (%)	Modulus (GPa)
PSMC Al-0.3Mn Alloy	72.3	20.4	28.9%	66.3
PSMC HP Al	59.2	14.0	37.1%	60.8

3.3. Tensile Behavior

3.3.1. Tensile properties

The typical engineering stress–strain curves from tensile testing of the PSMC Al-0.3Mn alloy and PSMC HP Al with a cross-sectional thickness of 10 mm are shown in Figure 7. Table 2 lists the tensile properties of the PSMC Al-0.3Mn alloy and HP Al. As shown in Figure 7, the slope of the linear portion of the engineering curve for the PSMC Al-0.3Mn alloy had a large increasing tendency than that of the PSMC HP Al. The UTS of the PSMC Al-0.3Mn alloy and PSMC HP Al were 72.3 MPa and 59.2 MPa, respectively, which signifies an improvement of 22% over that of the PSMC HP Al for the as-cast conditions. The yield strength of the PSMC Al-0.3Mn alloy was 20.4 MPa on average, which was 46% higher than that of the PSMC HP Al (14.0 MPa). However, the elongation of the PSMC Al-0.3Mn alloy was 28.9%, whereas the elongation of the PSMC HP Al (99.9%) was 37.1%, which had a decrease of 22% over that of the PSMC HP Al.

3.3.2. Resilience

The ability of a material to absorb energy is referred to as resilience when it is deformed elastically, and releases that energy upon unloading. The resilience is usually measured by the modulus of resilience which is defined as the maximum strain energy absorbed per unit volume without creating a permanent distortion. It can be calculated by integrating the stress-strain curve from zero to the elastic limit. In uniaxial tension, the strain energy per unit volume can be determined by the following equation [4, 16, 17]:

$$U_r = \frac{(YS)^2}{2E} \quad \text{(Eq 3)}$$

where U_r is the modulus of resilience, YS is the yield strength, and E is the Young's modulus. The calculated modulus of resilience for PSMC Al-0.3Mn alloy and PSMC HP Al (99.9%) are given in Table 3. In comparison between the PSMC Al-0.3Mn alloy and PSMC HP Al (99.9%), the modulus of resilience in the PSMC Al-0.3Mn alloy was 3.14 kJ/m^3 higher than that of the PSMC HP Al (99.9%) (1.61 kJ/m^3). As such, the PSMC Al-0.3Mn alloy was much more capable of resisting energy loads in engineering application during service, in which no permanent deformation and distortion are allowed.

3.3.3. Toughness

The tensile toughness of a ductile alloy is its ability to absorb energy during static loading condition, i.e., static deformation with a low strain rate. The ability to bear applied stresses higher than the yield strength without fracturing is usually required for various engineering applications. The toughness for ductile alloys can be considered as the total area under the stress-strain curve for the amount of the total energy per unit volume. To evaluate the deformation behavior, the energy expended in deforming a ductile alloy per unit volume given by the area under the stress-strain curve can be approximated by [4, 16]

$$U_t = U_{el} + U_{pl} = \frac{(YS+UTS)\times e_f}{2} \quad \text{(Eq 4)}$$

where U_t is the total energy per unit volume required to reach the point of fracture, U_{el} is the energy per unit volume for elastic deformation, U_{pl} is the energy per unit volume for plastic deformation, and e_f is the elongation at fracture. Table 3 lists the calculated U_t for the PSMC Al-0.3Mn alloy and PSMC HP Al (99.9%). The PSMC Al-0.3Mn alloy had a U_t value of 13.40 MJ/m^3, which was comparable to that (13.58 MJ/m^3) of the PSMC HP Al (99.9%). The total area under the engineering stress and strain curve of the PSMC Al-0.3Mn alloy was almost the same as that of the PSMC HP Al (99.9%). This was because the PSMC Al-0.3Mn alloy had the much higher ultimate tensile strength and yield strength, despite the PSMC HP Al (99.9%) having a very high elongation. Hence, the PSMC Al-0.3Mn alloy capable of absorbing the energy during deformation was as tough as the PSMC HP Al (99.9%).

Table 3. Tensile toughnesses and resiliences of PSMC Al-0.3Mn alloy and PSMC HP Al (99.9%) at room temperature

Material	Resilience (kJ/m^3)	Toughness (MJ/m^3)
PSMC Al-0.3Mn Alloy	3.14	13.40
PSMC HP Al	1.61	13.58

3.3.4. Strain Hardening

Figure 8 show the true stress vs. strain curves of the PSMC Al-0.3Mn alloy and PSMC HP Al. The true stress and strain for plastic deformation can be related by the power law equation:

$$\sigma_t = K\,\varepsilon_t^n \quad \text{(Eq 5)}$$

where σ_t is the true stress, ε_t is the true strain, K is the strength coefficient, and n is the strain-hardening exponent [17, 18]. The regression analysis indicated that the power expression agreed well with the tensile data. The numerical values of the derived constants in Eq (5) with the regression coefficients (R^2) are listed in Table 4. The high strain-hardening exponent implied that the PSMC Al-0.3Mn alloy would gain strength more quickly than the PSMC CP Al during plastic deformation.

To determine the strain-hardening rate ($d\sigma_t/d\varepsilon_t$), Eq (5) was differentiated to obtain:

$$d\sigma_t/d\varepsilon = K\,n\varepsilon_t^{n-1} \quad \text{(Eq 6)}$$

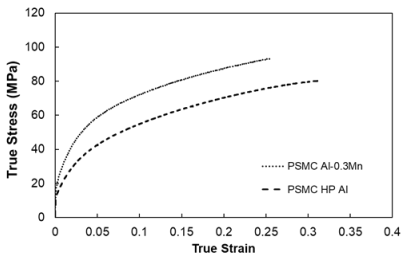

Fig. 8: True stress vs. strain curves

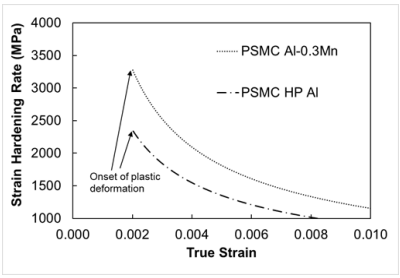

Fig. 9: Strain hardening curves

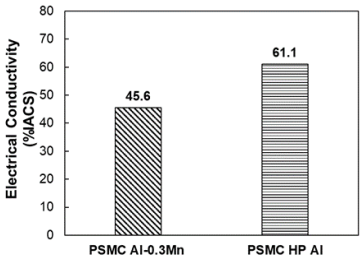

Fig. 10. Electrical conductivities

Figure 9 presents the strain-hardening rate versus true plastic strain curve during the plastic deformation, which was derived from the true stress versus true strain curve (Figure 8). Upon the onset of plastic deformation at a strain of 0.002, the strain-hardening rate of the PSMC Al-0.3Mn alloy was 3253 MPa, as the PSMC HP Al exhibited a strain-hardening rate of 2318 MPa. In the early stage of plastic deformation, the strain-hardening rate of PSMC Al-0.3Mn alloy was 40% higher than that of the PSMC HP Al. As the strain increased to 0.008, the strain-hardening rates of the PSMC Al-0.3Mn alloy and HP Al decreased to 1312 and 1007 MPa, respectively. At a strain of 0.008, the strain-hardening rate of the PSMC Al-0.3Mn alloy remained higher than that of the PSMC HP Al by 30%. An observation of the variation of strain-hardening rate versus strain suggested that, compared to the HP Al, the PSMC Al-0.3Mn alloy could strengthen itself spontaneously to a large degree upon plastic deformation. The high content of the imtermetallic phases in the microstructure of the PSMC Al-0.3Mn alloy should be responsible for the high tensile properties and strain hardening rate. The tensile behavior of the PSMC Al-0.3Mn alloy and HP Al generally agreed with the microstructural observation.

Table 4. Best fit parameters for power equations

Material	K (MPa)	n	R^2
PSMC Al-0.3Mn Alloy	165.17	0.3505	0.9962
PSMC HP Al	137.66	0.393	0.9988

3.4. Electrical Conductivities

The electrical conductivities of both the PSMC Al-0.3Mn alloy and PSMC HP Al are displayed in Figure 10. The electrical conductivity of the PSMC Al-0.3Mn alloy was 45.6 %IACS, while it was 61.1 %IACS for the PSMC HP Al (99.9%). There was a decrease of 25% in the electrical conductivity of the PSMC Al-0.3 Mn alloy compared to that of the PSMC HP Al. However, the conductivity of 45.6 %IACS was much higher than those (30 %IACS) of the commercially available Al casting alloys. The microstructure analyses indicated that the addition of 0.3 wt% Mn was primarily consumed in the formation of the Al-Mn intermetallic phase. As a result, a limited amount of Mn was dissolved in the primary Al, which made the Al electron movement almost unaffected in the Al-Mn solid solution. The minimum requirement of the electrical conductivity for the EV motor applications is about 48 %IACS [1]. The difference between the 48 and 45.6 %IACS is only 5%. The proper adjustment of the Mn content in Al-Mn solid solution should boost the electrical conductivity of Al-Mn alloy to meet the industrial specification. The similar phenomena taking place in the cast Al-Fe alloys [17, 18] and Mn-containing wrought Al alloys [19] were observed previously.

4. Summary

The results of tensile testing of the PSMC Al-0.3Mn alloy and HP Al showed that the UTS, YS and resilience of the PSMC Al-0.3Mn alloy were 72.3 and 20.4 MPa, and 3.14 kJ/m^3, respectively, which were higher than those (59.2 and 14.0 MPa, and 1.61 kJ/m^3) of the PSMC HP Al. The toughness of the PSMC Al-0.3Mn alloy was 13.40 MJ/m^3, which was comparable to that (13.58 MJ/m^3) of the PSMC HP Al. But, the elongation of the PSMC Al-0.3Mn alloy was only 28.9%, which was lower than that (37.1%) of the PSMC HP Al. The difference in tensile behavior between the PSMC Al-0.3Mn alloy and the HP Al should be attributed to the fact that the relatively large amount of the micron Al-Fe-Mn and nano Al-Mn intermetallic phases was present in the PSMC Al-0.3Mn alloy, compared to almost little intermetallic phase in the PSMC HP Al. The addition of 0.3 wt% Mn affected the electrical conductivity of the PSMC HP Al, which was only slightly below the industrial specification for the EV motor application.

Acknowledgements

The authors would like to thank the Natural Sciences and Engineering Research Council of Canada, Nemak, Ford Ford Motor Company of Canada, and University of Windsor for supporting this work

References

[1] Y. Li, A. Hu, Y. Fu, S. Liu, W. Shen, H. Hu and X. Nie, "Al Alloys and Casting Processes for Induction Motor Applications in Battery-Powered Electric Vehicles: A Review," *Metals*, vol. 12, pp.216-241, 2022.

[2] S. Liu, A. Hu, H. Hu, X. Nie and N.C. Kar, "Potential Al-Fe Cast Alloys for Motor Applications in Electric Vehicles: An Overview," *Key Eng. Mater*. Vol.923, pp. 3-19, 2022.

[3] M. Y. Murashkin, I., Sabirov, X., Sauvage, & R. Z. Valiev, "Nanostructured Al and Cu alloys with superior strength and electrical conductivity," *J Mater Sci*. Vol. 51(1), pp. 33-49, 2016.

[4] Y. Li, Y. Fu, A. Hu, X. Nie and H. Hu, "Effect of Sr and Ni Addition on Microstructure, Tensile Behavior and Electrical Conductivity of Squeeze Cast Al-6Si-3Cu Al Alloy," *Key Eng. Mater*. Vol.921, pp. 3-14, 2022.

[5] H. Ishikawa, Y. Takashima, Y. Okada, "Squirrel-Cage motor Rotor and Squirrel-Cage Motor." U.S. Patent 9 935 533, 2018.

[6] P. Sivanesh, K. Charlie, S.J. Robert, F. Ethan, E. Paul, "Aluminum Alloys for Die Casting." U.S. Patent 20210332461A1, 2021.

[7] S. W. Nam, D. H. Lee, "The effect of Mn on the mechanical behavior of Al Alloys." *Met. Maters*. Int. Vol. 6, no. 1 , pp. 13-16, 2000.

[8] A. J. McAlister, J. L. Murray, "The (Al-Mn) aluminum-manganese system - journal of phase equilibria." Bulletin of *Alloy Phase Diagrams* Vol. 8, no. 5 , pp. 438–447, 1987.

[9] J. Davis, ASM Specialty Handbook: *Aluminum and Aluminum Alloys*; ASM International, OH, USA, 2002.

[10] D. Beaulieu, *Characteristics of Structural Aluminum; Presses de l'aluminum: Chicoutimi*, QC, Canada, 2005.

[11] T. Bubonyi, P. Barkoczy. "Evaluation of Eutectic Structure in Aluminum Alloys." DOI:10.26649/musci.2019.073, MultiScience - XXXIII. microCAD International Multidisciplinary Scientific Conference, University of Miskolc, Borsod-Abauj-Zemplen, Hungary, 23-24 May, 2019.

[12] "Standard Test Method for Density of High-Modulus Fibers." D3800-99, *ASTM*, Vol 15.03, pp. 186-187, 2002

[13] "Standard Test Method for Dry and Wet Bulk Density, Water Absorption, and Apparent Porosity of Thin Sections of Glass-Fiber Reinforced Concrete," C948-81, ASTM Standards, *ASTM*, Vol 04.05, pp. 588-589, 2002.

[14] T.J. Collins, "ImageJ for Microscopy," Biotechniques, 43(1), S25–S30, 2007.

[15] "Standard Test Methods for Tension Testing Wrought and Cast Aluminum-and Magnesium-alloy Products," B557M, ASTM Standards, *ASTM*, Vol 02 02, 424-439, 2002.

[16] W.D. Callister and D.G. Rethwisch: *Materials Science and Engineering.* 10th edition, Wiley, USA, 2018.

[17] S. Liu, A. Hu, A. Dhaif, W. Shen, H. Hu. "Mechanical Properties and Electrical Properties of Permanent Mold Cast Eutectic Al-1.8Fe Alloy. Aluminum Alloys, Characterization and Processing." *TMS Annual Meeting & Exhibition, San Diego*, United States of America. In press, 2023.

[18] X. Wang, R.G. Guana, R.D.K. Misra, Y. Wang, H.C. Li, Y.Q. Shang, "The mechanistic contribution of nanosized Al3Fe phase on the mechanical properties." *Mater*. Sci. Eng A, vol. 724, pp. 452-460, 2018.

[19] R. M. Miri, "Effect of Manganese (Mn) Content and Homogenization Treatment on Hot Deformation of AA3xxx Aluminum Alloys, " Master Thesis, University of Waterloo, Waterloo, Ontario, Canada, 2016.